Synthesis, processing and properties of TaC–TaB$_2$–C ceramics

I.G. Talmy *, J.A. Zaykoski, M.M. Opeka

Naval Surface Warfare Center Carderock Division (NSWCCD), 9500 MacArthur Blvd., West Bethesda, MD 20817-5700, United States

Abstract

Multi-phase ceramics in the TaC–TaB$_2$–C system were prepared from TaC and B$_4$C mixtures by reactive pressureless sintering at 1700–1900 °C. The pressureless densification was promoted by the use of nano-TaC and by the presence of active carbon in the reaction products. The presence of TaB$_2$ inhibited grain growth of TaC and increased the hardness compared to pure TaC. If a coarse TaC powder was used, the compositions did not densify. In contrast, pure nano-TaC was pressureless sintered at 1800 °C by the addition of 2 wt.% carbon introduced as carbon black or graphite. The introduction of carbon black resulted in fully dense TaC ceramics at temperatures as low as 1500 °C. The grain size of nominally pure TaC ceramics was a strong function of carbon stoichiometry. Enhanced grain size in sub-stoichiometric TaC, compared to stoichiometric TaC, was observed. Additional work is necessary to optimize processing parameters and evaluate the properties of ceramics in the TaC–TaB$_2$–C system. Published by Elsevier Ltd.

Keywords: A. Sintering; B. Microstructure; D. Carbides; D. Carbon; D. Borides

1. Introduction

The group IV–VI transition metal borides, carbides, and nitrides with melting temperatures close to or above 3000 °C are potential candidates for ultra high-temperature (UHT) applications such as hypersonic vehicles (leading edges and nose-caps) and propulsion components. These applications require materials capable of operating at temperatures exceeding 2000 °C with unique mechanical and thermochemical properties, high strength, fracture toughness, and oxidation resistance.[1]

At this time, there are no off-the-shelf materials to meet the future application needs. The selection and development of potentially suitable structural materials for use at UHT conditions is needed. Single-phase non-oxide ceramics are significantly limited in these UHT applications due to poor thermal shock and oxidation resistance. Multi-phase materials, either ceramic–ceramic or ceramic–metal (cermets), can combine advantageous properties of each of the composing phases, significantly modify microstructure and properties, provide the potential for their tailoring, and broaden the application spectrum. The system TaC–TaB$_2$–C, which is the subject of the present study, includes components with melting temperatures of 3983 and 3037 °C, for TaC and TaB$_2$, respectively, and for

carbon a sublimation temperature of about 3700 °C all of which can provide promising multi-phase materials for the UHT applications.

The TaC–TaB$_2$–C system is a part of the Ta–C–B ternary system in the range of compositions bounded by three pseudo-binary systems: TaC–TaB$_2$, TaB$_2$–C, and TaC–C. Rudy et al. investigated phase relations in the Ta–C–B system, which were presented as an isothermal section at 1750 °C.[2] Phase relations in the TaB$_2$–TaC system were studied by Ordan'yan et al.[3,4] The constructed phase diagram had a eutectic at 2730 °C at the composition containing 34 wt.% TaC. No mutual solubility between the end members was determined below 2100 °C. About 7 wt.% TaB$_2$ was dissolved in TaC at the eutectic temperature. A eutectic with the absence of significant mutual solid solubility was reported by Levinskii et al.[5] for the TaB$_2$–C system at 2650 °C and 32 mol% TaB$_2$, while Glaser[6] and Rudy et al.[2] reported stability in the TaB$_2$ + C mixtures up to 2900 °C. In the Ta–C phase diagram modified by Wiesenberger et al.,[7] the high carbon phase boundary of TaC$_{1-x}$ was given at 49.8 at.% C and the TaC$_{1-x}$–C eutectic at 61 at.% C and 3445 °C.

It has to be noted that B$_4$C, which is also a component of the Ta–C–B ternary system, is not chemically compatible with Ta or TaC. It reacts with Ta and TaC forming TaB$_2$ and free carbon that has been used for the synthesis and processing of diboride-containing ceramics.[8–11,17,19] There are no literature data on ceramics containing all three components and very lim-

* Corresponding author.
E-mail address: inna.talmy@navy.mil (I.G. Talmy).

1. REPORT DATE **2010**	2. REPORT TYPE	3. DATES COVERED **00-00-2010 to 00-00-2010**

4. TITLE AND SUBTITLE **Synthesis, processing and properties of TaC-TaB2-C ceramics**	5a. CONTRACT NUMBER
	5b. GRANT NUMBER
	5c. PROGRAM ELEMENT NUMBER
6. AUTHOR(S)	5d. PROJECT NUMBER
	5e. TASK NUMBER
	5f. WORK UNIT NUMBER

7. PERFORMING ORGANIZATION NAME(S) AND ADDRESS(ES) **Naval Surface Warfare Center Carderock Division (NSWCCD),9500 MacArthur Blvd,West Bethesda,MD,20817-5700**	8. PERFORMING ORGANIZATION REPORT NUMBER

9. SPONSORING/MONITORING AGENCY NAME(S) AND ADDRESS(ES)	10. SPONSOR/MONITOR'S ACRONYM(S)
	11. SPONSOR/MONITOR'S REPORT NUMBER(S)

12. DISTRIBUTION/AVAILABILITY STATEMENT
Approved for public release; distribution unlimited

13. SUPPLEMENTARY NOTES

14. ABSTRACT
see report

15. SUBJECT TERMS

16. SECURITY CLASSIFICATION OF:			17. LIMITATION OF ABSTRACT	18. NUMBER OF PAGES	19a. NAME OF RESPONSIBLE PERSON
a. REPORT **unclassified**	b. ABSTRACT **unclassified**	c. THIS PAGE **unclassified**	**Same as Report (SAR)**	**11**	

ited data on the preparation and properties of ceramics in the pseudo-binary systems TaC–TaB$_2$, TaC–C, and TaB$_2$–C.

Tantalum monocarbide (TaC$_x$) exists in a wide range of carbon-deficient stoichiometries where x can range from 0.72 to 0.99.[12–15] Carbon diffusivity increased with decreasing carbon content. It was found that the carbon diffusion rate at 1700 °C was approximately six times higher in sub-stoichiometric TaC$_{0.77}$ than in stoichiometric tantalum carbide.[14]

Alexandre et al.[15] evaluated mechanical properties of monolithic TaC$_{0.80}$ prepared by HIPing of Ta/TaC mixtures at 1900 K and 195 MPa for 2 h. The flexural strength and fracture toughness of the ceramics were 281 ± 5.5 MPa and 3.6 ± 0.4 MPa m$^{1/2}$, respectively.

Since both densification and grain growth in ceramics are controlled by diffusion, it can be expected that densification and grain size in carbon-deficient TaC, would be different than those in stoichiometric tantalum carbide.

Recent publications of Missouri S&T[16–18] describe research centered on the densification of TaC by hot pressing in the presence of TaB$_2$ and B$_4$C. The relative density of the samples containing 10 wt.% TaB$_2$ was 98.6% after hot pressing at 2100–2200 °C compared to 85–89% for pure TaC hot pressed at 2300 °C. The presence of TaB$_2$ enhanced the mechanical properties of the ceramics.[16] The TaB$_2$-containing TaC ceramics were also prepared with the addition of 1 and 2 wt.% B$_4$C. The formation of TaB$_2$ and carbon as a result of chemical reaction between TaC and B$_4$C promoted densification and inhibited crystal growth. The ceramics achieved relative density of 98% after hot pressing at 2100 °C. The Vickers hardness of the TaB$_2$-containing ceramics was higher than that of pure TaC ceramics.[17]

The introduction of the additives consisting of 0.43 wt.% B$_4$C with 0.13 wt.% carbon resulted in 98% relative density after hot pressing at 2200 °C compared to 96% for pure TaC hot pressed at 2400 °C. The densifying effect was attributed to the removal of oxide impurities from grain boundaries.[18]

Composites in the TaC-(20–66.7) mol% TaB$_2$ systems were also prepared by self-propagating high-temperature synthesis in Ta–B$_4$C–C and Ta–B$_4$C mixture compacts.[18] Results showed that the reaction temperature and propagation velocity of the combustion front depended on the boride phase content. The synthesized products were porous with 15–30 μm grains of spherical or irregular shape.

The microhardness of the TaC–TaB$_2$ ceramics measured by Ordan'yan et al.[3] changed from 18 GPa for pure TaC to 23 GPa for pre-eutectic compositions and was 26–27 GPa for all post-eutectic ones. Tkachenko[20] determined that the wear resistance of TaC–TaB$_2$ ceramics was much higher than that of each compound separately.

All materials in the previously described publications were prepared using hot pressing. Due to strong covalent bonding and low self-diffusion coefficients, pressureless densification of TaC and TaB$_2$ is very difficult at reasonable temperatures without sintering aids.

Pressureless densification of carbides in the presence of carbon (introduced directly or formed in situ as a result of chemical reactions) has been reported for B$_4$C ceramics, which, simi-

larly to other non-oxides, cannot be densified without external pressure or addition of sintering aids. Sub-micron powders of B$_4$C were densified[21] by pressureless sintering to 97% relative density at about 2200 °C by the addition of 4–12 wt.% carbon. Grain growth during sintering was inhibited by the increase in carbon content. Radev and Zahariev[22] reported the activation of B$_4$C sintering by the addition of group IV–VI transition metal carbides. The reaction between these carbides and B$_4$C during high-temperature processing, with the formation of borides and active carbon, accelerated diffusion processes in the bulk and along grain boundaries of the phases.

U.S. Pat. No. 4,195,066[23] describes pressureless densification of sub-micron B$_4$C to at least 90% theoretical density at 2100–2200 °C by the addition of 0.1–8 wt.% carbon black, graphite or phenolic resin. During processing the resin was converted by pyrolysis to amorphous carbon. Sigl and Schwetz[24] accomplished pressureless sintering of B$_4$C up to 97% relative density by the addition of carbon black. The presence of carbon resulted in retardation of crystal growth and a resulting grain size below 2 μm.

Sigl et al. patented[25] a process for producing B$_4$C ceramics containing MB$_2$ (M = Ti, Zr, Hf, V, Nb and Ta) and carbon by reacting B$_4$C (surface area 5–50 m^2/g) with the corresponding monocarbides. The monocarbides were added in the amounts necessary to form 2 to 6 wt.% free carbon during subsequent sintering. For these compositions, 4–13 vol.% MB$_2$ was formed. The ceramics were pressureless sintered to a relative density of 92% at 2100–2250 °C. The MB$_2$ had a grain-growth-inhibiting effect that also promoted sintering. Subsequent HIPing without encapsulation was used if higher density was required.

The present paper reports the results of ongoing research proceeding in two directions. First, on the synthesis, processing, and characterization of multi-phase ceramics in the TaC–TaB$_2$–C system using a displacement reaction between TaC and B$_4$C, and second, on the densification of TaC in the presence of different forms of carbon (carbon black and graphite).

2. Experimental procedure

Reactions (1)–(5) used to synthesized TaC–TaB$_2$–C ceramics are given below:

$$2TaC + B_4C \rightarrow 2TaB_2 + 3C \tag{1}$$

$$4TaC + B_4C \rightarrow 2TaC + 2TaB_2 + 3C \tag{2}$$

$$8TaC + B_4C \rightarrow 6TaC + 2TaB_2 + 3C \tag{3}$$

$$12TaC + B_4C \rightarrow 10TaC + 2TaB_2 + 3C \tag{4}$$

$$16TaC + B_4C \rightarrow 14TaC + 2TaB_2 + 3C \tag{5}$$

The materials obtained as a result of these five reactions were identified as 2:1, 4:1, 8:1, 12:1, and 16:1, respectively, in the text, tables, and figures.

Sub-micron TaC (identified in the text also as nano or fine) powder (99.9% purity and 100 nm particle size, according to manufacturer's data sheet) was purchased from Atomergic Chemetals Corp, Plainview, NY in 1976. The company does

Table 1
Composition of starting materials and calculated content (in vol.% and wt.%) of the reaction products in TaC–B$_4$C mixtures.

TaC:B$_4$C ratio and sample identification	Wt.% B$_4$C in raw mixtures	Volume% of reaction products			Weight% of reaction products		
		TaC	TaB$_2$	C	TaC	TaB$_2$	C
2:1	12.5	0	67	33	0	91.83	8.17
4:1	6.65	35	42.5	22.5	46.6	49.0	4.4
8:1	3.45	62	25	13	72.4	25.3	2.25
12:1	2.3	73.8	17.6	8.6	81.4	17.1	1.5
16:1	1.75	79.9	13.4	6.7	85.95	12.9	1.15

not exist any more, and no information about the method used for preparation of the powder could be found. The stoichiometry of the powder was TaC$_{0.97}$ (determined by Laboratory Testing Inc., Hatfield, PA and in NSWCCD by XRD). The powder had surface area of 11.74 m^2/g (measured in NSWCCD by BET, Micromeritics ASAP 20010, Norcross, GA) and contained 3.02 wt.% oxygen (determined by Laboratory Testing Inc., Hatfield, PA). XPS analysis (Dr. A. Mansour, NSWCCD) showed that some oxygen is present as Ta$_2$O$_5$.

The coarse TaC powder (99.5% purity, −325 mesh) was purchased from CERAC Inc. Specialty Inorganics (Milwaukee, WI). The B$_4$C powder (99.4% purity, 1–7 μm particle size) was purchased from Alfa Aesar (Ward Hill, MA) and had surface area of 4.84 m^2/g (determined in NSWCCD by BET). TaB$_2$ (99.5% pure; −325 mesh) was purchased from CERAC Inc. and carbon black (surface area about 25 m^2/g) from Cabot Corporation (Boston, MA). Two graphite powders with surface area of 3.0 and 8.0 m^2/g were purchased from Superior Graphite Co. (Chicago, IL).

The powders with no additional grinding were mixed with the mortar and pestle in acetone. The mixing procedure was repeated three times with intermediate drying. The samples were prepared by cold pressing (Carver Inc., 3850, Wabash, IN) in a steel mold at 100 MPa followed by cold isostatic pressing (CIP'ing; Fluitron, Ivyland, PA) at about 300 MPa. The pressed samples were pressurelessly sintered in an Astro Model 1000-2560 furnace (Thermal Technology, Santa Barbara, CA) in a He atmosphere or vacuum at temperatures in the range of 1500–2100 °C with a hold up to 2 h.

The fired samples were characterized by density and open porosity (Archimedes principle), shrinkage, phase composition (X-ray diffraction, Siemens Theta/Theta, Model D 500, Bruker AXS, Madison, WI), and microstructure (SEM, Model ISI ABT SR-50A, Withington, Manchester, UK). Energy dispersive spectroscopy (EDS) was also used to identify the elemental composition of phases.

The lattice constant, a, of TaC prepared under different conditions, was determined using EVA software (Bruker, Madison, WI) and used to calculate C/Ta ratio, X, from the equation:[12]
$X = 6.398\,a - 27.516$.

The mechanical properties were characterized by 3-point flexural strength (Instron Model 8562, Canton, MA), crosshead motion was 0.5 mm/min**,** and Vickers hardness under 1 kg load (Leco, Model V-100-C2, St. Joseph, MI). The bars (25 mm × 3 mm × 2.5 mm, 20 mm span) for strength measurements were cut from the sintered disks, edge beveled at 45°, final

polished with 6 μm diamond grit. The strength and hardness data were typically the average of five and ten measurements, respectively.

The thermodynamic data from Schick[25] and "JANNAF"[26,27] were used to calculate free energy changes and adiabatic temperatures (T_{ad}) for all the reactions.

3. Results and discussion

3.1. Ceramics in the TaC–TaB$_2$–C system

The composition of starting materials and calculated content of reaction products are given in Table 1. The table shows that the content of TaC in the final ceramics increases and TaB$_2$ and carbon decreases with increasing TaC content in starting materials. The calculated volumes of the reactants and reaction products were approximately equal for all the reactions excluding contraction or expansion of the samples unrelated to the reactions or sintering.

Thermodynamic calculations were performed to determine the free energy and enthalpy changes for reactions (1)–(5). The Gibbs free energy change for reaction (1), calculated with an assumption of unit activities for the reactants and products, is negative up to 4040 K, indicating that the reaction proceeds in the forward direction as shown. The Gibbs free energy does not change with the excess of TaC. Using the enthalpy of formation data, reaction (1) was found to be exothermic with an adiabatic reaction temperature of 3373 K. Energy balances computed for reactions (1)–(5), using the enthalpy data from the same sources, reveal the significant reduction in the adiabatic reaction temperatures with increasing TaC content in the reactants as shown in Table 2.

The XRD patterns of the nano and coarse TaC powders, shown in Fig. 1, did not reveal any noticeable differences indicating that the amount of oxygen-containing compounds in the nano-TaC (oxygen content 3.02 wt.%) was below the range

Table 2
Adiabatic temperatures of reactions for TaC + B$_4$C mixtures.

Reactants	Products	Adiabatic temp. (K)
2TaC + B$_4$C	2TaB$_2$ + 3C	3373
4TaC + B$_4$C	2TaC + 2TaB$_2$ + 3C	2525
8TaC + B$_4$C	6TaC + 2TaB$_2$ + 3C	1760
12TaC + B$_4$C	10TaC + 2TaB$_2$ + 3C	1397
16TaC + B$_4$C	14TaC + 2TaB$_2$ + 3C	1182
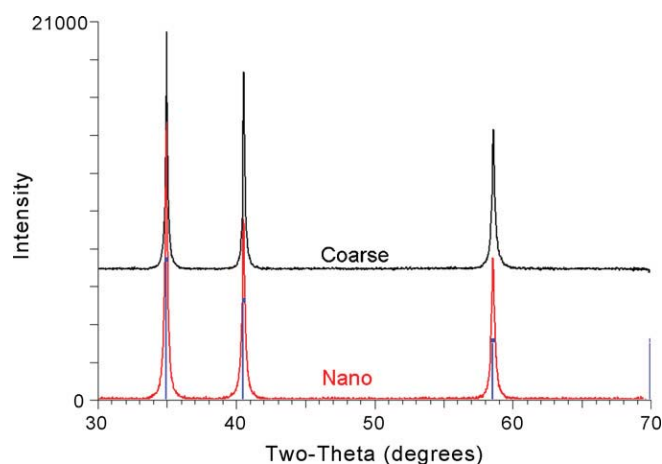
Fig. 1. XRD of TaC powders (nano and coarse).

Fig. 3. Open porosity of ceramics prepared from nano-TaC/B_4C mixtures by pressureless sintering as a function of composition and temperature.

identifiable by XRD. However, calculations showed that, if all oxygen was consumed to form Ta_2O_5, the oxide content would be as high as 16.6 wt.% (10.8 vol.%), and XRD should detect it. This suggests that oxygen could be dissolved in the TaC crystal lattice to a significant degree, but this explanation does not seem likely because TaC XRD peaks were not shifted from the standard positions.

Fig. 2 shows the XRD patterns of the 2:1 ceramics based on nano-TaC after firing at 1500, 1700, and 1900 °C in He for 2 h. The final products of reaction (1) should contain only TaB_2 and carbon. However, the sample fired at 1500 °C contained residual TaC indicating that the reaction did not go to completion at this temperature. It was practically completed at 1700 °C. Firing in vacuum intensified the process, and the reaction was completed at 1500 °C (XRD not shown). Additionally, no carbon (graphite) peaks were identified in the samples after processing at the above temperatures (calculated C content in the material is 8.17 wt.%, see Table 1) indicating that carbon may be present in the amorphous form.

The open porosity and shrinkage of the nano-TaC-based ceramics in the whole range of compositions are shown in Figs. 3 and 4. The ceramics were prepared by pressureless sin-
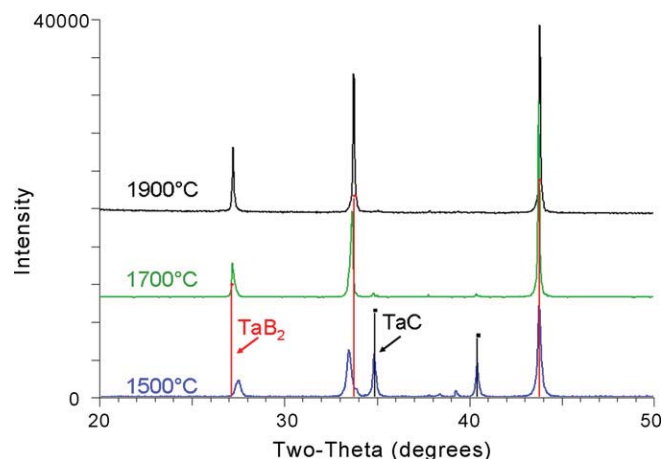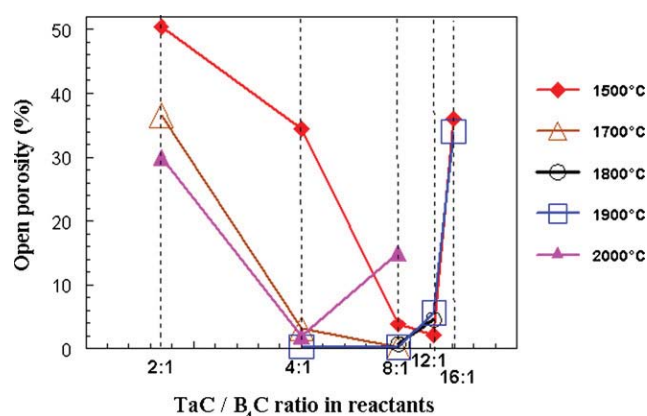
tering at 1500–2000 °C in He for 2 h. Fig. 3 reveals a very significant difference in sinterability as a function of composition creating porosity "valley". The 2:1 and 16:1 materials were not densified at any test temperature and showed expansion (11 and 4%, respectively) after firing at 1500 °C. For the 2:1 ceramics, the expansion can be related to the highly exothermic nature of reaction (1), which could proceed according to the pattern of self-propagating high-temperature synthesis.[28,29] Combustion reactions in freestanding samples result in high porosity in the final part, which can be associated with internal pressure created by the expulsion of volatile materials during reaction.[19,29,30] By analogy with B_4C,[25] the poor sinterability of the 16:1 composition could be due to the insufficient amount of carbon released in reaction (5) for densification of the ceramics (1.3 wt.% related to TaC, see Table 1). The sample showed 34% open porosity and only 2.25% shrinkage after firing at 1900 °C.

The 4:1 ceramics were densified by pressureless sintering above 1700 °C. However, at 1500 °C the material showed very low degree of densification with about 34.5% open porosity and 1% shrinkage. These values were changed to 3 and 24.5%, respectively, in the temperature range from 1500 to 1700 °C. The low degree of densification at 1500 °C could be related to the competing expansion from the occurrence of the combustion reaction at these temperatures. Although the T_{ad} was seldom

Fig. 2. XRD of the 2:1 ceramics after firing at 1500, 1700, and 1900 °C for 2 h in He.
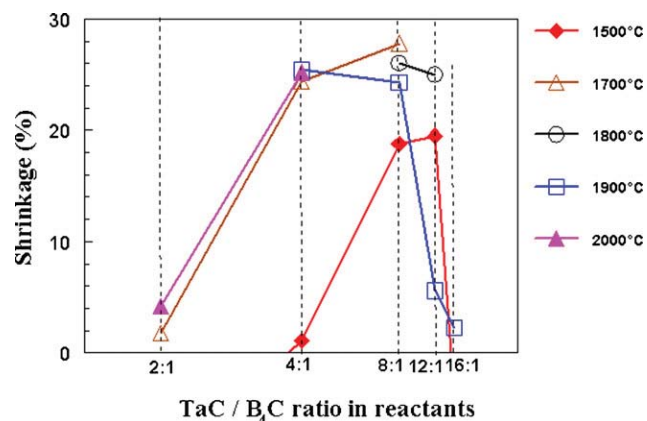
Fig. 4. Shrinkage of ceramics prepared from nano-TaC/B_4C mixtures by pressureless sintering as a function of composition and temperature.
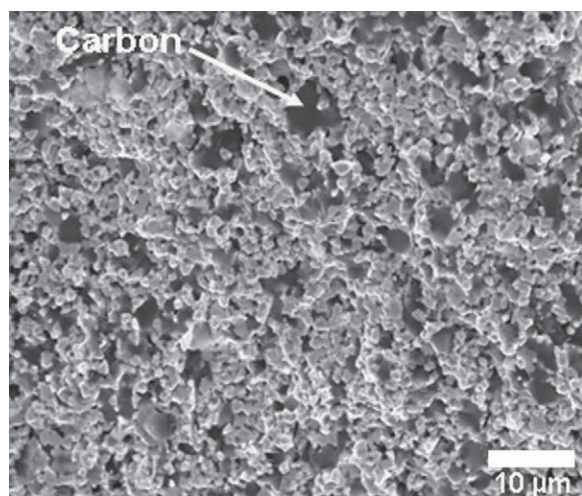
5

Fig. 5. SEM of 2:1 ceramics prepared by pressureless reaction sintering at 1900 °C for 2 h in He.

achieved because of heat losses to the surroundings, the temperature of 2525 K (Table 2) for reaction (2) was high enough to assume the combustion process occurred.

Compared to the previous compositions, the 8:1 and 12:1 ceramics exhibited a high degree of densification yielding an open porosity below 5% and shrinkage close to 20% even after firing at 1500 °C. For these materials with T_{ad} of 1760 and 1397 K, respectively, the self-sustaining combustion reactions would be impossible. It was suggested[30] that self-sustaining combustion reactions could not proceed if T_{ad} were equal or below 1800 K. The open porosity of the 8:1 ceramics fired at 2000 °C was 15.0% compared to 0.2% after firing at 1900 °C, which was due to over firing.

The SEM micrograph of 2:1 ceramics (Fig. 5) displays a porous two-phase material consisting of TaB_2 with grain size below 2 μm and carbon (dark phase), which was not detected by XRD as previously mentioned. Fig. 6 shows the SEM micrographs of the fracture surfaces of the 4:1, 8:1, and 12:1 ceramics prepared from nano-TaC-based mixtures by sintering at 1900 °C for 2 h in He. The microstructure of all three materials was very uniform with predominantly transgranular type of fracture and a grain size below 5 μm increasing with decreasing TaB_2 and C contents. The presence of carbon was easily identified only in the 4:1 ceramics with the calculated carbon content of 22.5 vol.%. The grain size also increased with increasing firing temperature in the 1700–1900 °C temperature range as shown in Figs. 7 and 8 for 4:1 and 8:1 ceramics. It is important to note that oxygen content in the 8:1 ceramics fired at 1800 °C was only 0.036 wt.% indicating a significant removal of oxygen-containing species during processing in the presence of carbon released as a reaction product and present in a furnace atmosphere.

Several experiments were carried out to determine the specific characteristics of the starting components and/or reaction products leading to pressureless densification of the ceramics. The main goal was to identify the role of the particle size of starting TaC and the role of carbon, both its crystallinity and particle size. The reactant side of Eq. (3) only gave the possibility to explore the effect of TaC particle size since carbon formed as a
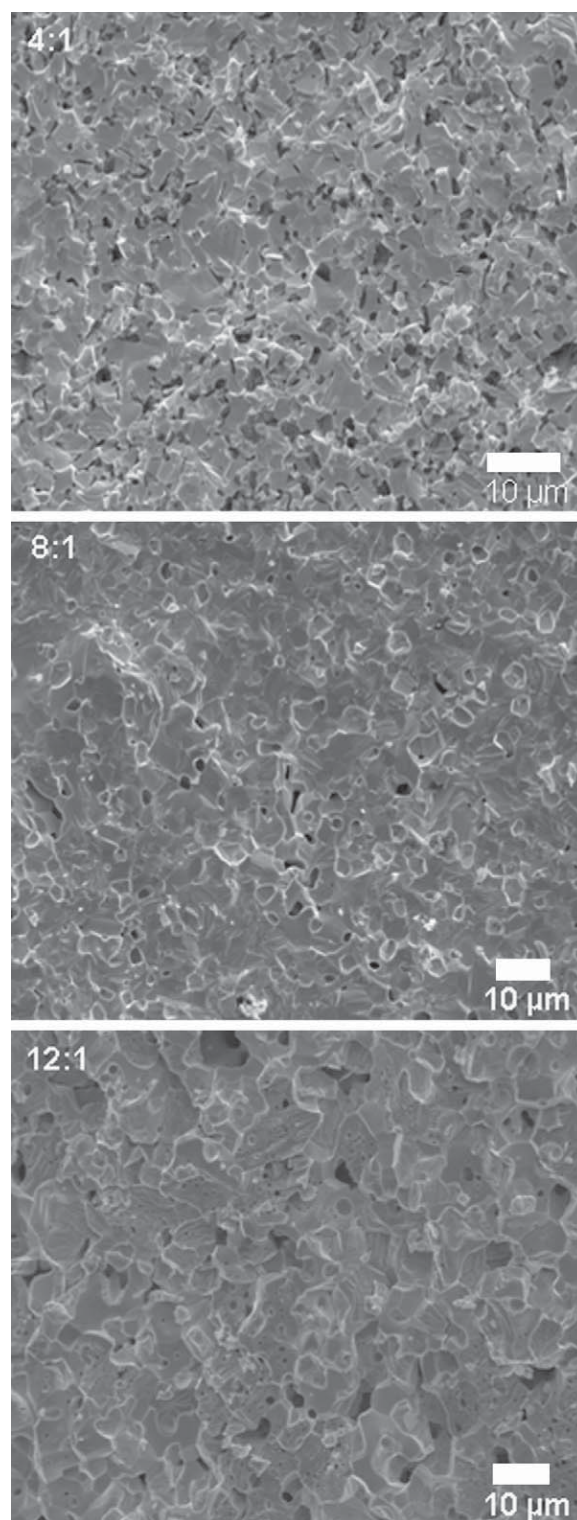

Fig. 6. SEM of TaC–TaB_2–C ceramics (4:1, 8:1 and 12:1) prepared by pressureless sintering at 1900 °C for 2 h in He.

product of the chemical reaction, and its crystallinity and particle size upon formation could not be identified. Because of that, the 8:1 ceramics were also prepared from the mixture of the final products of reaction (3): $6TaC + 2TaB_2 + 3C$. These nonreactive mixtures offered the possibility to explore the effect of
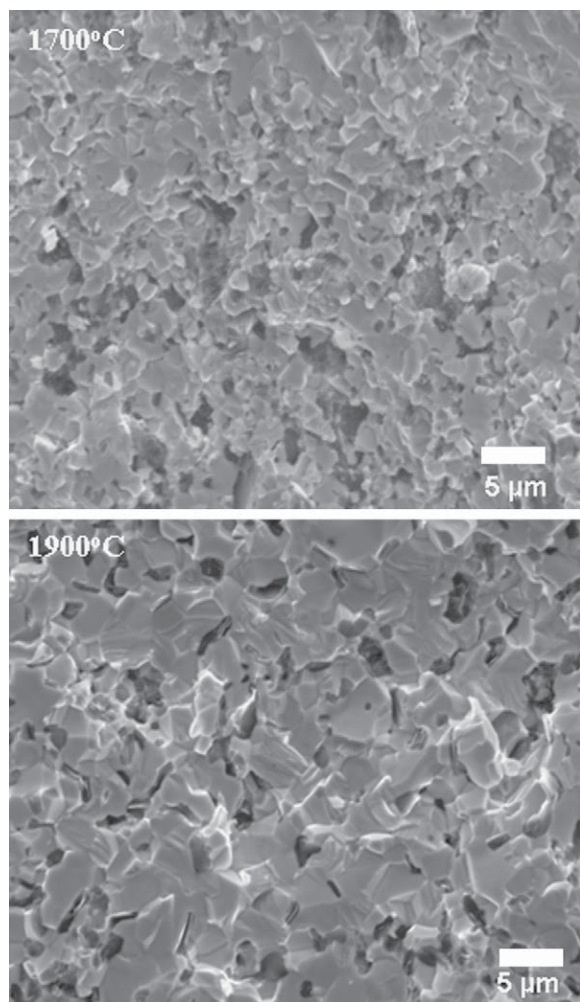
6 *I.G. Talmy et al. / Journal of the European Ceramic Society xxx (2010) xxx–xxx*

Fig. 7. SEM of 4:1 ceramics prepared by pressureless sintering at 1700 and 1900 °C for 2 h in He.

Fig. 8. SEM of 8:1 ceramics prepared by pressureless sintering at 1700, 1800, and 1900 °C for 2 h in He.

crystallinity and particle size for both TaC and carbon on the densification of ceramics. Thus, reactive and non-reactive sintering occurred in the mixtures based on the left and right sides of reaction (3), respectively. Tantalum diboride powder (−325 mesh) was used in all the experimental compositions. The resulting data are summarized in Table 3.

The use of coarse TaC instead of nano-TaC in both the reactive and non-reactive starting mixtures resulted in ceramics with open porosities of 42 and 32%, respectively, after firing at 2100 °C, confirming the critical role of the TaC particle size. The use of nano-TaC and carbon black in the non-reactive mixtures also resulted in fully dense ceramics after pressureless sintering at 1800 °C. The elimination of carbon from the nano-TaC-based non-reactive mixture resulted in 19% porosity after firing at 1800 °C. The use of graphite (surface area of 3 and 8 m^2/g) instead of carbon black did not lead to pressureless densification of the non-reactive mixture and resulted in an open porosity of about 27% regardless of graphite powder surface area. The experiments conclusively showed that both nano-TaC and carbon black are required for pressureless densification of TaC–TaB$_2$–C ceramics regardless of the type of starting mixture compositions (reactive or non-reactive) used in the present study.
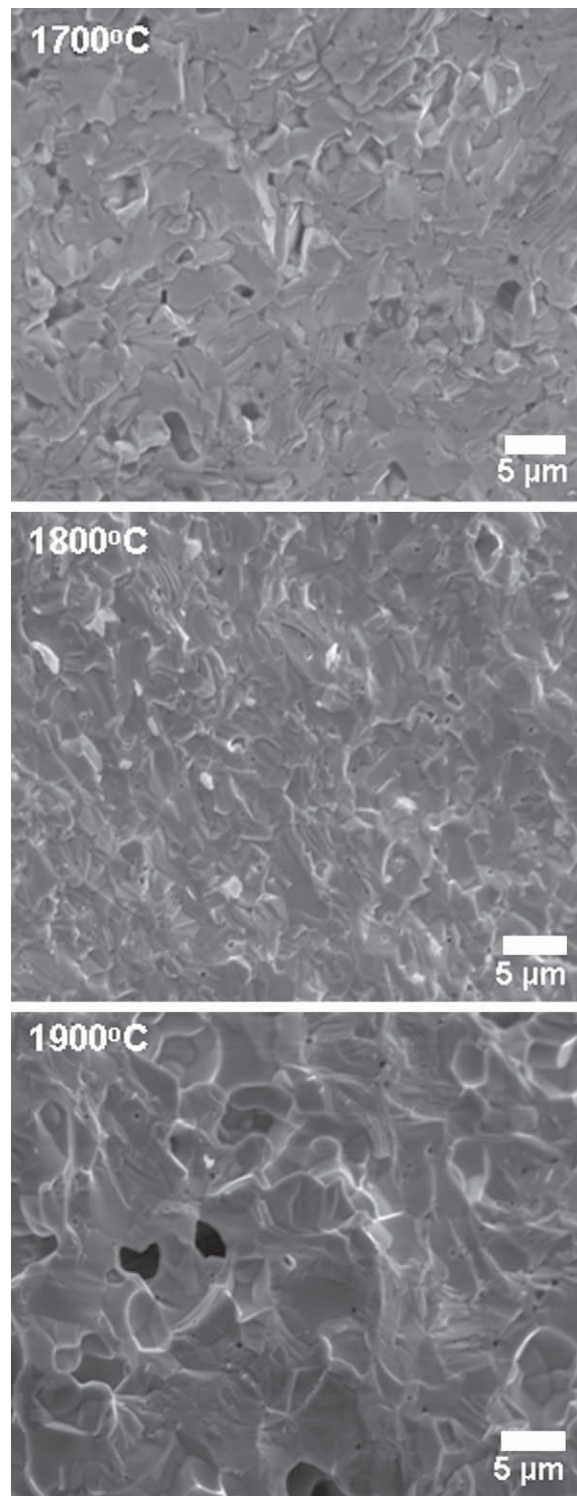
The SEM micrographs of the fracture surfaces of the fully dense 8:1 ceramics, prepared using nano-TaC-based reactive and non-reactive starting mixtures, are shown in Fig. 9. The ceramics from the non-reactive mixture displayed a coarser microstructure compared to ceramics based on the reactive mixture. Both materials exhibited a transgranular fracture behavior.

Table 3
Open porosity of 8:1 ceramics as a function of types of starting compositions, TaC powder particle size, and carbon form.

TaC	Carbon type	Processing temperature (°C)	Open porosity (%)
Reactive processing from $8TaC + B_4C$ mixture			
Nano	Reaction carbon	1800	0
Coarse	Reaction carbon	2100	42
Non-reactive processing from $6TaC + 2TaB_2 + 3C$ mixture			
Nano	Carbon black	1800	0
Nano	Graphite, $3 \, m^2/g$	1800	27
Nano	Graphite, $8 \, m^2/g$	1800	28
Nano	No carbon	1800	19
Coarse	Carbon black	2100	32

At the present time, flexural strength and Vickers hardness were measured only for the fully dense 8:1 ceramics from both reactive and non-reactive mixtures that were pressureless sintered at 1900 and 1850 °C, respectively. The values of strength and hardness were 220 ± 30 MPa and 22.2 GPa, respectively, for the ceramics from the reactive mixtures, and 383 ± 2.5 MPa and 23.9 GPa, respectively, for the ceramics from the non-reactive mixtures.

The smaller particle size of ceramics derived from the reactive mixture (Fig. 9) should result in a higher room temperature strength compared to that of the larger-particle size ceramics derived from the non-reactive mixture. The data showed the opposite trend, which could be attributed to residual stresses developed in the material as a result of in situ formation of TaB_2 and carbon. An annealing of the samples is in the future plan to investigate this hypothesis.
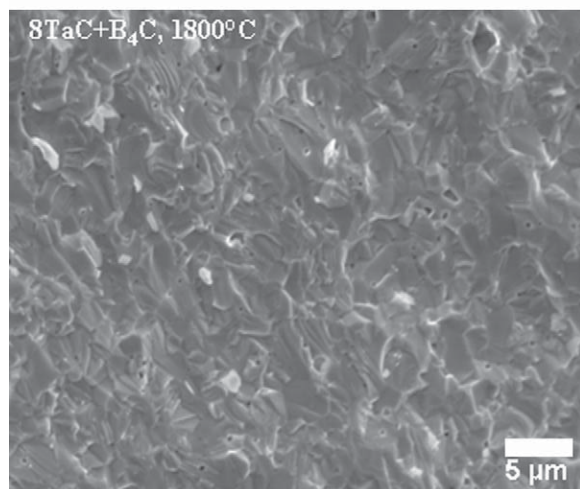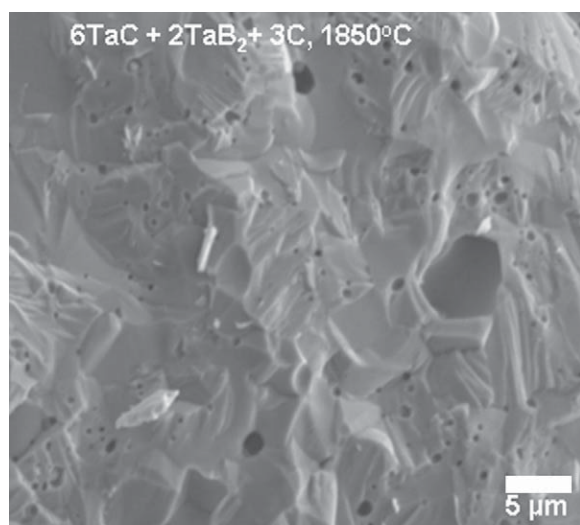

Fig. 9. SEM of TaC–TaB_2–C ceramics prepared from $8TaC + B_4C$ (reactive) and from $6TaC + 2TaB_2 + 3C$ (non-reactive) mixtures by pressureless sintering.
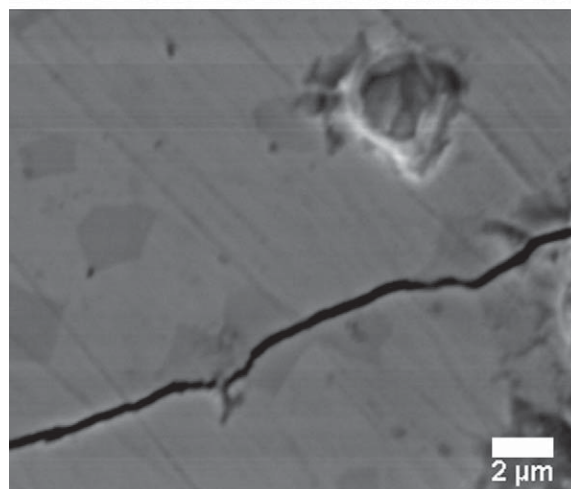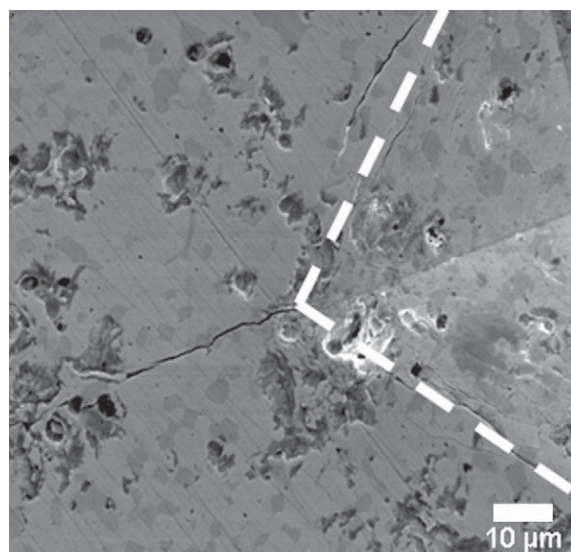

Fig. 10. SEM of an indent (10 kg load) in 8:1 ceramics pressureless sintered at 1900 °C (dashed line shows the corner of the indent).
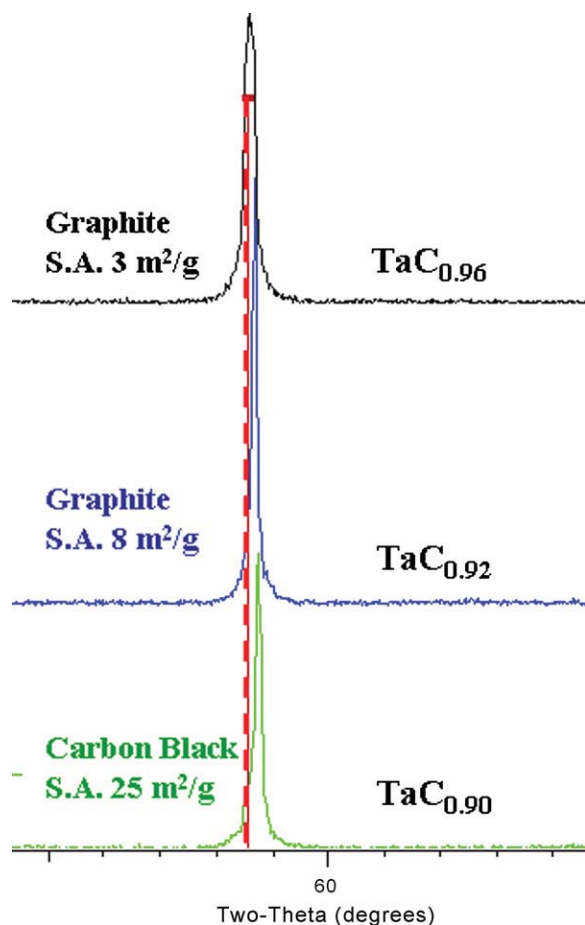
Fig. 11. XRD of nano-TaC–2 wt.% C ceramics pressureless sintered at 1800 °C in vacuum as a function of carbon form showing the shift of the (2 2 0) peak position and the corresponding TaC stoichiometry.

The hardness of the 8:1 ceramics was high for both processing methods due to the presence of 25 vol.% TaB_2. The measured values are in agreement with other reported data.[3,16,17] The Vickers indentation (10 kg load) produced a relatively straight crack propagation path (Fig. 10) without a significant crack deflection.

From these experiments and the results reported by Ordan'yan et al.[3] and Missouri S&T,[16–18] the presence of TaB_2 in TaC–TaB_2–C ceramics inhibited grain growth of TaC and enhanced their mechanical properties.

3.2. Densification of TaC in the presence of different forms of carbon

Pure nano-TaC without carbon additions had an open porosity of 19% after firing at 2100 °C. As mentioned above, the presence of both nano-TaC and carbon black were critical for densification of TaC–TaB_2–C ceramics. The effect of carbon on the sintering behavior of pure nano-TaC was investigated by the addition of 2 wt.% of three types of carbon: carbon black, and two graphite powders with surface areas of 3 and 8 m^2/g. The amount of carbon was selected to be close to that in the 8:1 non-reactive mixture (Table 3), which was sintered to full density at 1850 °C in the presence of carbon black. Samples were heated at
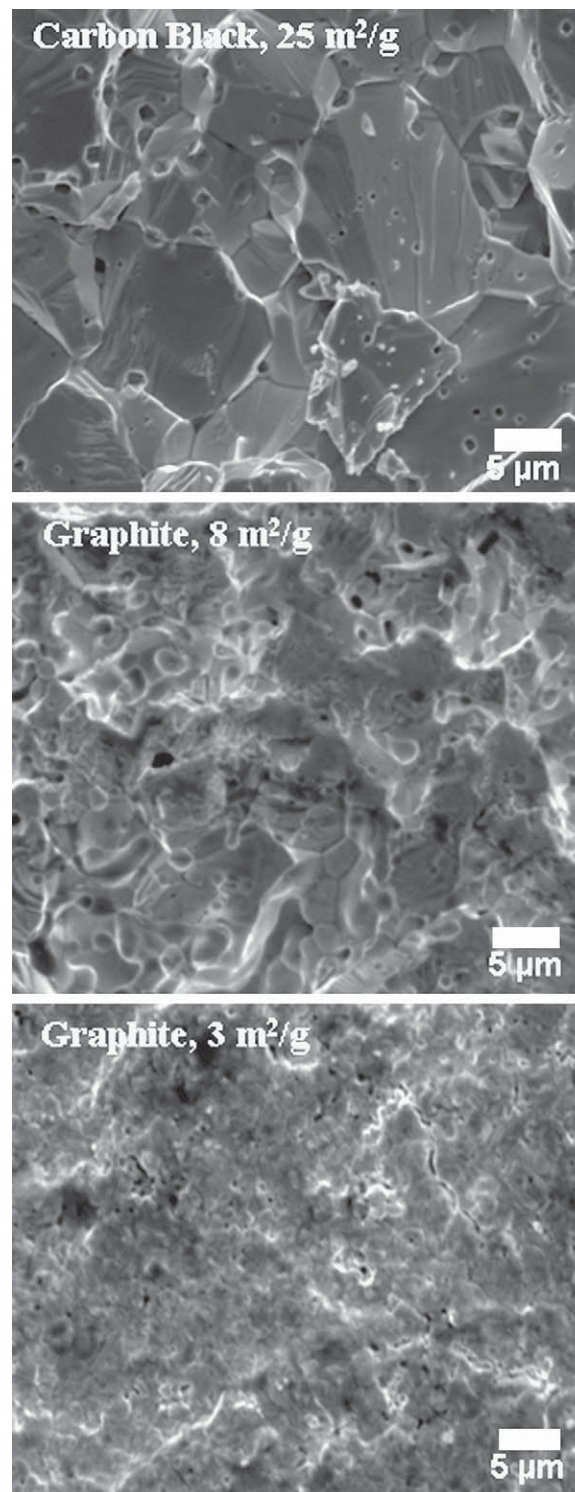

Fig. 12. SEM of nano-TaC + 2 wt.% carbon ceramics pressureless sintered at 1200 °C (1 h) followed by 1800 °C (2 h) in vacuum.

1200 °C for 1 h in vacuum to allow for oxygen removal, and then at 1800 °C for 2 h in vacuum for densification. All three samples, regardless of the types of carbon, were practically dense exhibiting negligible open porosity.

X-ray diffraction patterns of these samples (Fig. 11) show a shift in the position of the TaC diffraction peaks as a func-
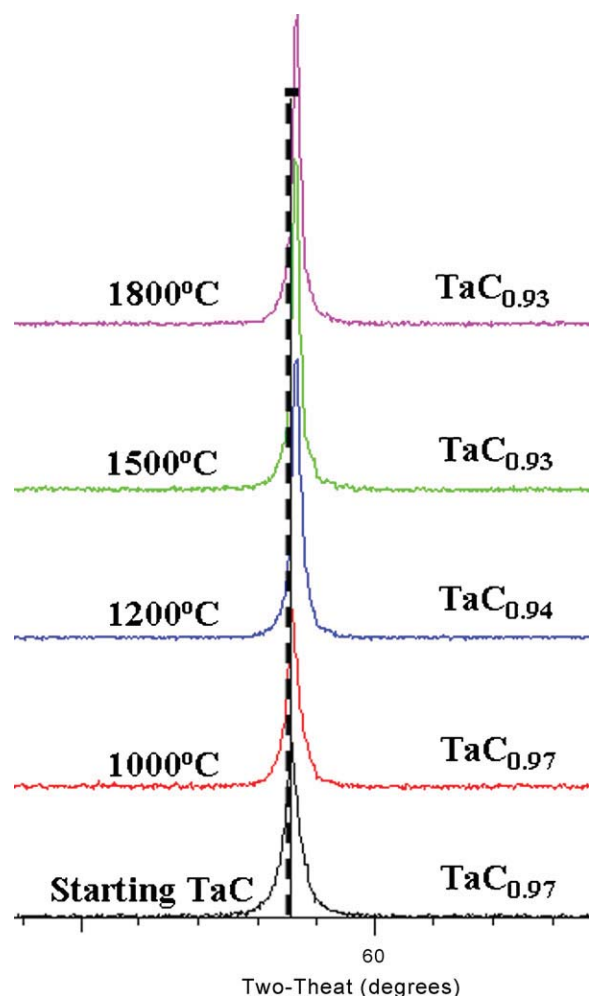
Fig. 13. XRD of nano-TaC–2 wt.% carbon black ceramics after pressureless sintering at 1000–1800 °C in vacuum showing the shift of the (2 2 0) peak position and the corresponding TaC stoichiometry.

tion of the particle size of starting carbon powders. The shift in diffraction peaks corresponded to a change in carbon stoichiometry of TaC, which decreased from $TaC_{0.96}$ to $TaC_{0.92}$ for ceramics prepared using graphite powders with the surface area of 3 and 8 m^2/g, respectively, and further decreased to $TaC_{0.90}$ when carbon black was used.

Fig. 12 shows micrographs of the fracture surfaces of the samples sintered with carbon black and graphite powders. The grain size of the final TaC was significantly affected by particle size of the starting carbon and, correspondingly, by the carbon stoichiometry in TaC. The sample prepared with carbon black had the lowest carbon content ($TaC_{0.90}$) and the largest grain size (5–15 μm), while the samples sintered in the presence of graphite had much finer microstructures, with a grain size decreasing with increasing graphite particle size and carbon content. Thus, carbon stoichiometry was primarily responsible for the microstructure of tantalum carbide, enhancing grain growth with increasing degree of sub-stoichiometry.

The phenomenon of enhanced grain growth in sub-stoichiometric carbides was reported for other carbide systems.
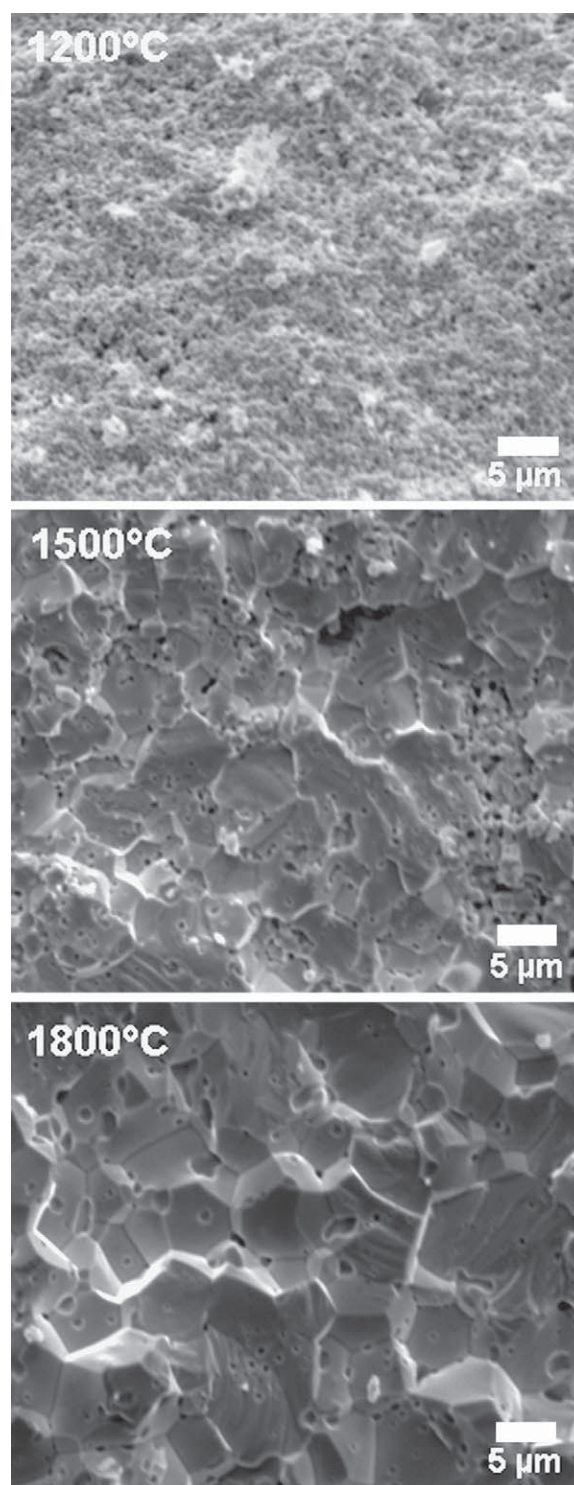

Fig. 14. SEM of nano-TaC + 2 wt.% carbon black ceramics pressureless sintered at 1200, 1500, and 1800 °C for 1 h in vacuum.

Rangaraj et al. reported[31] that the use of fine powders and sub-stoichiometric ZrC played the predominant role in densification of ZrB_2–ZrC composites significantly decreasing the temperature of reaction hot pressing. The Van Loo group[32] attributed enhanced densification of composites containing non-stoichiometric TiC and ZrC to the higher diffusivity of carbon
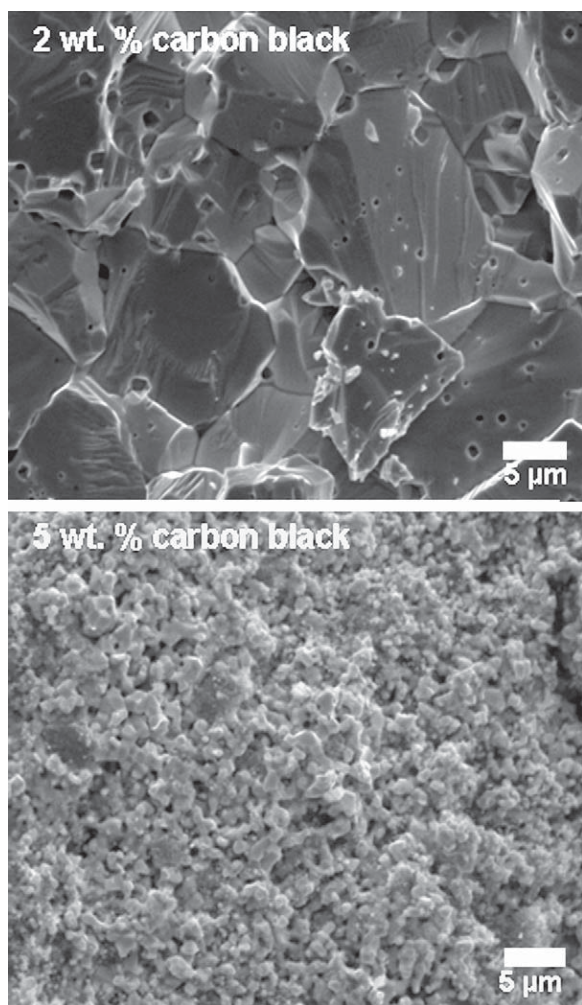
Fig. 15. SEM of nano-TaC with 2 and 5 wt.% carbon black pressureless sintered at 1200 °C (1 h) followed by 1800 °C (2 h) in vacuum.

in non-stoichiometric carbides compared to stoichiometric ones. Wuchina et al.[33] observed a significantly coarser microstructure in hot-pressed ceramics based on $HfC_{0.67}$ compared to those based on $HfC_{0.99}$.

A change in carbon stoichiometry was also observed for samples from mixtures of nano-TaC and 2 wt.% carbon black, which were fired at a series of temperatures from 1000 to 1800 °C for 1 h in vacuum. X-ray diffraction patterns of these samples (Fig. 13) showed a shift in the position of the TaC diffraction peaks as a function of temperature. The stoichiometry of $TaC_{0.97}$ for the starting powder did not change to 1000 °C, but then decreased to $TaC_{0.94}$ after heating at 1200 °C and to $TaC_{0.93}$ after heating at 1500 °C remaining unchanged after heating at 1800 °C.

Fig. 14 shows micrographs of the fracture surfaces of samples heated at 1200, 1500, and 1800 °C for 1 h. The ceramics fired at 1200 °C were porous with a sub-micron grain size. The ceramics heated at 1500 °C were dense with predominant grain size of about 5 μm. However, the samples still contained fine grain areas located mostly at the grain boundaries of the coarser grains. A longer hold at this temperature would result in a homogenizing of the microstructure. The heat treatment at 1800 °C yielded

fully dense ceramics with a very uniform microstructure and average grain size of about 5 μm. This enhancement of grain growth and densification of TaC with increasing temperature is likely related to the carbon stoichiometry and carbon diffusivity in TaC.

The addition of 5 wt.% carbon black to nano-TaC resulted in ceramics with an open porosity of 22% after two-step pressureless sintering in vacuum at 1200 °C for 1 h and 1800 °C for 2 h. Fig. 15 shows the dramatic difference in microstructure between the samples with 2 and 5 wt.% carbon black. Very insignificant grain growth occurred in ceramics processed with 5 wt.% carbon black, which displayed sub-micron grains, while the ceramics processed with 2 wt.% carbon black contained 10–20 μm grains. The difference in microstructure could be attributed to the presence of excess carbon at grain boundaries that interfered with crystal growth.

4. Conclusions

- Dense ceramics containing (in vol.%) 35–73.8 TaC, 25–62 TaB_2, and 8.6–22.5 carbon were prepared by reactive pressureless sintering of sub-micron powders at 1700–1900 °C.
- The pressureless densification of the TaC-based ceramics was promoted by the presence of active carbon in the reaction products. The use of nano-TaC and carbon black also led to pressureless densification of the $6TaC–2TaB_2–3C$ non-reactive mixture of the reaction products for the $8TaC/B_4C$ reaction.
- The presence of TaB_2 in the ternary ceramics inhibited grain growth of TaC and increased the hardness compared to pure TaC.
- Pure nano-TaC was pressureless densified at 1800 °C by the addition of 2 wt.% carbon introduced as carbon black or graphite. The presence of carbon black resulted in fully dense TaC ceramics even at 1500 °C. None of the compositions used in this study densified when the coarse TaC powder used.
- A very important conclusion from the present study is that the grain size of nominally pure TaC ceramics is a strong function of carbon stoichiometry. Enhanced grain size in sub-stoichiometric TaC, relative to stoichiometric TaC, was observed.
- Additional work is necessary to optimize processing parameters and evaluate the properties of ceramics in the $TaC–TaB_2–C$ system.

Acknowledgements

References

1. Opeka MM, Talmy IG, Zaykoski JA. Oxidation-based materials selection for 2000 °C+ hypersonic aerosurfaces: theoretical considerations and historical experience. *J Mater Sci* 2004;**39**(19):5887–904.

2. Rudy E, Benesovsky F, Toth L. Studies of ternary systems of the group Va and VIa metals with boron and carbon (in German). *Z Metallkd* 1963;**54**:345–53.

3. Ordan'yan SS, Unrod VI, Polishchuk VS, Storonkina NM. Interaction in the TaC–TaB$_2$ system. *Poroshk Metall* 1976;**165**(9):40–3.

4. Ordan'yan SS. Laws of interaction in the systems M^{IV,V}C–M^{IV,V}B$_2$. *Inorg Mater* 1980;**16**(8):961.

5. Levinskii YV, Salibekov SE, Levinskaya MK. Interections of diborides of V, Nb, Ta with carbon (in Russian). *Poroshk Metall (Kiev)* 1965;**5**(11):66–9.

6. Glaser FW. Contribution to the metal–carbon–boron systems. *Trans AIME: J Met* 1952;**4**:391–6.

7. Wiesenberger H, Lendauer W, Ettmayer P. Reaction diffusion and phase equilibria V–C, Nb–C, Ta–C and Ta–N systems. *Acta Mater* 1998;**46**(2):451–666.

8. Thomson R. Production, fabrication, and uses of borides. In: Freer R, editor. *The physics and chemistry of carbides, nitrides and borides*. Dordrecht: Kluwer Academic Publishers; 1990. p. 113–20.

9. Lundström T. Transition metal borides. In: Markovich VI, editor. *Boron and refractory borides*. Berlin: Springer-Verlag; 1977. p. 351–76.

10. Zhang GJ, Ando M, Yang JF, Ohji T, Kanzaki S. Boron carbide and nitride as reactants for in situ synthesis of boride-containing ceramic composites. *Eur Ceram Soc J* 2004;**2**:171–8.

11. Krylov YI, Bronnikov VA, Krysina VG, Pristavko VV. Possibilities of producing thermite mixtures based on B$_4$C–metal and SiC–metal composites. *Poroshk Metall* 1975;**12**(156):57–60.

12. Resnick R, Seigle L. The diffusion of carbon in tantalum monocarbide. *Trans AIME* 1966;**236**:1732–8.

13. Bowman AL. The variation of lattice parameter with carbon content of tantalum carbide. *J Phys Chem* 1961;**65**(9):1596–8.

14. Rafaja D, Lengauer W, Wiesenberger H. Non-metal diffusion coefficients for the Ta±C and Ta±N systems. *Acta Mater* 1998;**46**(10):3477–83.

15. Alexandre N, Desmaison M, Valin F, Boncoeur M. Solid state reaction between tantalum (Ta) and tantalum carbide powders (TaC) powders during HIPing. *Key Eng Mater* 1997;**132–136**:868–71.

16. Zhang X, Hilmas GE, Fahrenholtz WG. Densification, mechanical properties, and oxidation resistance of TaC–TaB$_2$ ceramics. *Am Ceram Soc J* 2008;**91**(12):4129–32.

17. Zhang X, Hilmas GE, Fahrenholtz WG. Densification and mechanical properties of TaC-based ceramics. *Mater Sci Eng A* 2009;**501**(1–2):37–43.

18. Zhang X, Hilmas GE, Fahrenholtz WG, Deason DM. Hot pressing of tantalum carbide with and without sintering additives. *Am Ceram Soc J* 2007;**90**(2):393–401.

19. Yeh CL, Chen YL. An experimental study on self-propagating high-temperature synthesis in the Ta–B$_4$C system. *J Alloys Compd* 2009;**478**(1–2):163–7.

20. Tkachenko YG. High-temperature friction and wear of eutectic carboboride alloys of group V metals. *Powder Metall Met Ceram* 1977;**16**(10):781–4.

21. Dole SL, Prochazka S. Densification and microstructure development in boron carbide. *Ceram Eng Sci Proc* 1985;**6–7**:8.

22. Radev D, Zahariev Z. Oxidation stability of B$_4$C–Me$_X$B$_Y$ composite materials. *J Alloys Compd* 1980;**197**:87–90.

23. Schwetz KA, Vogt G. Process for the production of dense sintered shaped articles of polycrystalline boron carbide by pressureless sintering, US Patent 4,195,066 (1980).

24. Sigl LS, Schwetz KA. Pressureless sintering of boron carbide with carbon black. In: *Proc. 2nd European Ceramic Soc. Conf.*. 1991. p. 517–21.

25. Sigl L, Thaler H, Schwetz KA. Process for producing bodies based on boron carbide by pressureless sintering, US Patent 5,505,899 (1996).

26. Schick HL, editor. *Thermodynamics of certain refractory compounds*, vol. II. New York/London: Academic Press; 1966.

27. JANAF termochemical tables, 2nd ed., Project Directors D.R. Stull and H. Prophet, NSRDS-NBS 37, 1971.

28. Munir ZA, Anselmi-Tamburini U. Self-propagating exothermic reactions: the synthesis of high-temperature materials by combustion. Materials science report, vol. 3, North-Holland, Amsterdam: Elsevier Science Publishers; 1989: p. 277–365.

29. Munir ZA. Synthesis of high-temperature materials by self-propagating combustion methods. *Am Ceram Bull* 1988;**67**(2):342–9.

30. Rice RW, McDonough. Intrinsic volume changes of self-propagating synthesis. *J Am Ceram Soc* 1985;**68**(5):C122–3.

31. Rangaraj L, Suresha SJ, Divakar C, Jayaram V. Low temperature processing of ZrB2–ZrC composites by reactive hot pressing. *Metall Mater Trans A* 2008;**39**(7):1496–505.

32. Van Loo FJJ, Wakelkamp W, Bastin GF, Metselaar R. Diffusion of carbon in TiC$_{1-y}$ and ZrC$_{1-y}$. *Solid State Ionics* 1989;**32–33**:824–32.

33. Wuchina E, Opeka M, Causey S, Buesking K, Spain J, Cull A, et al. Designing for ultrahigh-temperature applications: the mechanical and thermal properties of HfB$_2$, Hfc$_X$, HfN$_X$ and αHf(N). *J Mater Sci* 2004;**39**(19):5939–49.